

Improving Camouflaged Object Detection with the Uncertainty of Pseudo-edge Labels

Nobukatsu Kajiura
kajiura@nii.ac.jp
The University of Tokyo
National Institute of Informatics
Tokyo, Japan

Hong Liu
hliu@nii.ac.jp
National Institute of Informatics
Tokyo, Japan

Shin'ichi Satoh
satoh@nii.ac.jp
National Institute of Informatics
The University of Tokyo
Tokyo, Japan

ABSTRACT

This paper focuses on camouflaged object detection (COD), which is a task to detect objects hidden in the background. Most of the current COD models aim to highlight the target object directly while outputting ambiguous camouflaged boundaries. On the other hand, the performance of the models considering edge information is not yet satisfactory. To this end, we propose a new framework that makes full use of multiple visual cues, *i.e.*, saliency as well as edges, to refine the predicted camouflaged map. This framework consists of three key components, *i.e.*, a pseudo-edge generator, a pseudo-map generator, and an uncertainty-aware refinement module. In particular, the pseudo-edge generator estimates the boundary that outputs the pseudo-edge label, and the conventional COD method serves as the pseudo-map generator that outputs the pseudo-map label. Then, we propose an uncertainty-based module to reduce the uncertainty and noise of such two pseudo labels, which takes both pseudo labels as input and outputs an edge-accurate camouflaged map. Experiments on various COD datasets demonstrate the effectiveness of our method with superior performance to the existing state-of-the-art methods.

KEYWORDS

Uncertainty, camouflaged object detection, pseudo-edge/map synthesis, CVAE, camouflaged map refinement

1 INTRODUCTION

Camouflage is a way for creatures in nature to blend into the surroundings to make it harder for preys and predators to notice themselves [4]. Camouflaged Object Detection (COD) is a task of detecting objects from images containing such camouflaged objects [9], as shown in the first column of Figure 1. COD is expected to have a wide range of applications, including ecological protection, medicine, surveillance systems, search and rescue systems for disaster, military applications, anomaly detection [9]. In addition, it is expected that improving the accuracy of COD would improve the accuracy of generic object detection.

COD is a more challenging task compared to generic object detection [22]. This is because the foreground has a similar texture to the background, which is not easy for a human to notice the camouflaged object [38]. In existing COD methods [8, 9], due to the boundaries of camouflaged objects are not clear enough, they often result in blurred and ambiguous boundaries of the output camouflaged map. Inspired by [5, 30], making good use of edge information is helpful for performance improvement. However, the

performance of recent models [39, 44], that consider edge information, achieve lower performance than regular COD models like [8]. Therefore, we aim to integrate the edge information into the process of COD, which is to refine the predicted camouflaged maps by referring to the separately predicted edges.

In this paper, we propose a new framework, called **Uncertainty Reduction COD** (UR-COD), that explicitly considers the edge information of the camouflaged object, which is to enhance the current COD model by introducing a camouflaged edge detection module and to output camouflaged map with clear defined boundary (as shown in Figure 1). The proposed framework can extract powerful features that identify more details of camouflaged objects than models that do not or implicitly consider the boundaries of camouflaged objects. In particular, we first introduce a camouflaged edge detection module, in which output edge is used as a pseudo-edge label. Second, we use a conventional COD model to generate the coarse camouflaged map that can be seen as a pseudo-map label. Consequently, our goal is to generate an accurate camouflaged map by given the pseudo-edge label and pseudo-map label. However, these pseudo labels are noisy and contain uncertainty compared to ground-truth labels. To this end, we use the Conditional Variational Auto-encoder (CVAE) [35] to build an uncertainty-aware map refinement module, which can output a camouflaged map even in the presence of noisy pseudo label inputs. It is worth noting that our framework can use any existing COD models as the pseudo-map generator, and our proposed uncertainty-enhanced model consistently improves the performance of the original model. The whole framework of our proposed model is shown in Figure 2.

To verify the usefulness of our method, quantitative evaluation is conducted on the CAMO dataset [20], CHAMELEON dataset [34], COD10K dataset [9], and NC4K dataset [27]. The results demonstrate that our framework outperforms the corresponding conventional COD methods in almost all of the four widely-used evaluation metrics, which are S-measure [6], E-measure [7], weighted F-measure [28], and MAE. Furthermore, it is shown that the best performing COD model exceeded the performance of the state-of-the-art model when used as a pseudo-map generator.

Our main contributions are summarized as follows:

- We explicitly consider uncertain camouflaged edge and camouflaged map information and improve the conventional COD methods.
- Experiments on various COD datasets confirm that the performance of our method outperforms that of the conventional state-of-the-art methods.

2 RELATED WORK

2.1 Camouflaged Object Detection

Previous COD methods can be categorized into either low-level-features-based methods or deep-features-based methods. Low-level-features-based methods are methods for detecting camouflaged objects based on low-level features, such as color, shape, and brightness of the image. There are many methods for this research [11, 16, 19, 25, 31–33, 36], but their performance is not yet satisfactory. This is because a well-performed camouflage is good at deceiving low-level features, so it is difficult to detect camouflaged objects using low-level features. To solve this problem, deep-features-based methods have been attracting attention in recent years.

Deep feature-based methods use deep neural networks to correctly output the camouflaged maps from an input image during training, and predict the camouflaged maps of the objects during testing. Le et al. [20] proposed ANet that addressed both classification and segmentation tasks. Fan et al. [8, 9] introduced SINet and SINet-v2 that first roughly searched for camouflaged objects and then identified their segments. Yan et al. [43] proposed MirrorNet that focused on instance segmentation and adversarial attack. Sun et al. [39] proposed C²FNet, which integrated the cross-level features with the consideration of rich global context information. Mei et al. [29] proposed PFNet via the distraction mining strategy. Lyu et al. [27] introduced camouflaged object discriminative region localization and camouflaged object ranking. Zhang et al. [46] introduced RGB-D COD with a monocular depth estimation network. According to the current leaderboard¹, SINet-v2 has shown particularly high performance that directly segments objects, while the boundaries of the output camouflaged map are often ambiguous.

On the other hand, some methods focus on edge information of camouflaged objects. Wang et al. [40] used edge information to improve the performance of salient object detection. Zhu et al. [51] proposed TINet, which interactively refined multi-level texture including contour edge and Canny edge [2]. Zhai et al. [44] introduced a graph-based joint learning framework for detecting camouflaged objects and edges.

Though these deep-features-based methods show considerably higher performance than low-level-features-based methods, methods that segment objects directly have the problem of edge clarity, while methods that consider edges have the problem of accuracy. Therefore, to overcome these problems, we aim to combine the best of both methods and propose to refine the directly predicted camouflaged maps by referring to the separately predicted edges. Moreover, to solve the problem of the low performance of edge-based methods, our method takes into account the uncertainty of the predicted edges.

2.2 Edge detection

With the development of deep learning, many high-performance edge detection methods have been proposed [1, 24, 37, 42]. However, most of the objects in the datasets handled by these methods are general salient objects, and they do not provide sufficient performance for camouflaged objects. Gu et al. [13] proposed CENet that uses a UNet-based model for improving the medical image

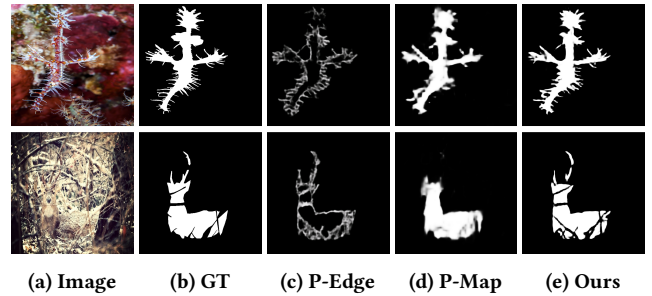


Figure 1: Illustration of the proposed method. "P-" represents a pseudo label, and our method outputs edge-accurate camouflaged maps based on the uncertain pseudo-map labels and pseudo-edge labels. Note that any conventional COD method can be used as the pseudo-map generator (PMG), and state-of-the-art SINet-v2 [8] is used here.

segmentation. This method extracts semantic information of the context and generates a high-level feature map by using dense atrous convolution (DAC) blocks [13] and residual multi-kernel pooling (RMP) blocks [13]. Therefore, compared to other methods that do not consider semantic information, this method is likely to be applicable even when the detection target is not salient.

2.3 Uncertainty-aware object detection

Existing methods for object detection treat saliency map prediction as a point estimation problem by learning the correspondence between input images and ground-truth maps, which deterministically generate a single saliency map. However, since ground-truth map labels are based on human annotations, especially in the field of salient object detection, the recognition of the most salient objects differs among annotation generators, and the ground-truth labels themselves contain uncertainty. Zhang et al. [45] solved this problem of label uncertainty by using a Conditional Variational Auto-encoder (CVAE) [35], that is called UCNet. UCNet introduces CVAE to model uncertainty of human annotation, and accurate object detection is achieved. In our proposed method, we generate pseudo labels for camouflaged maps and edges to obtain accurate COD. Since the pseudo labels are generated by a learning-based method, there is some uncertainty in the pseudo labels. To address this problem, it is necessary to consider the uncertainty.

3 METHOD

The purpose of this study is to predict camouflaged maps with well-defined boundaries from an input image containing camouflaged objects. In conventional COD methods, there lacks a model that takes the edge information into account while the camouflaged map output is often wrong or the boundary is ambiguous and blurred. Therefore, we introduce a camouflage edge detection module that explicitly estimates the boundary while accounting for the uncertainty, and we call this new framework as **uncertainty-reduction COD (UR-COD)**. As shown in Figure 2, our framework consists of three modules: pseudo-map generator (PMG) (in Sec.3.1), pseudo-edge generator (PEG) (in Sec.3.2), and uncertainty-aware map refinement (UAMR) module (in Sec.3.3). The details of each module are described below.

¹<http://dpfan.net/Camouflage/>

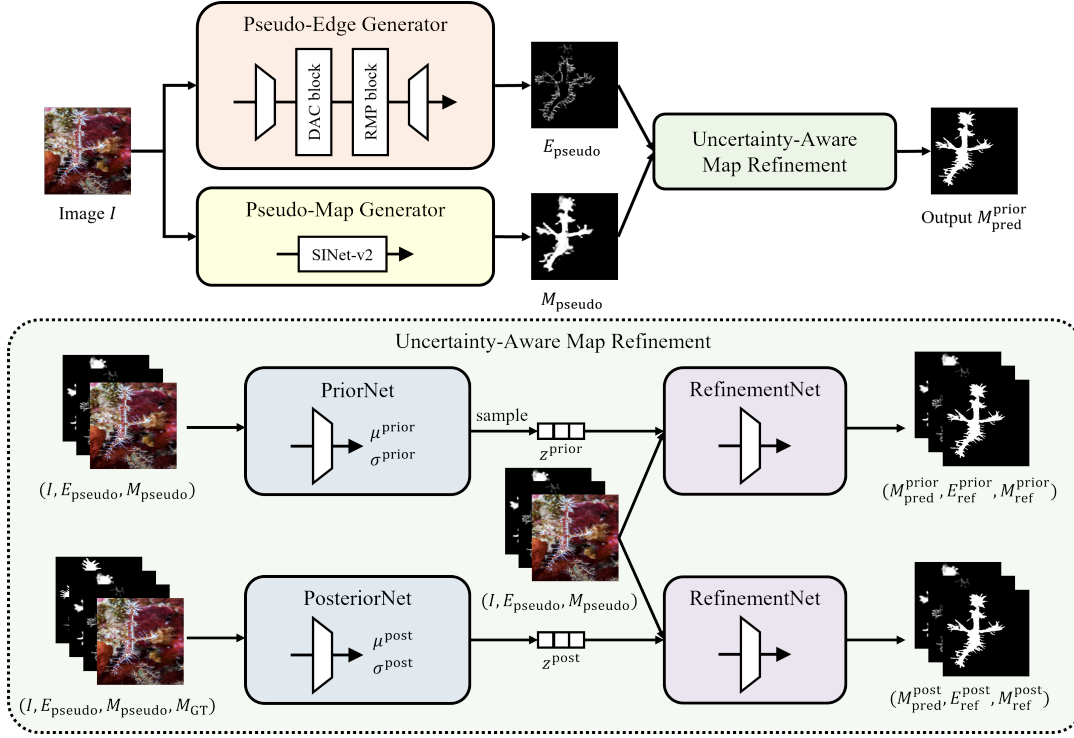


Figure 2: Overview of our framework. The obscure boundaries of pseudo-map labels generated by the pseudo-map generator (PMG) are refined by the uncertainty-aware map refinement (UAMR) module using pseudo-edge labels generated by the pseudo-edge generator (PEG).

3.1 Pseudo-Map Generator (PMG)

The output camouflaged map generated by the conventional COD methods often has unclear boundaries. In this method, a coarse camouflaged map is generated from the RGB image I using the conventional COD method, and it is treated as a pseudo-map label M_{pseudo} . In other words, PMG is a module that outputs a pseudo-map label M_{pseudo} from an RGB image I . In this paper, we chose five methods as baselines for the COD models: SiNet [9], SiNet-v2 [8], PraNet [10], C²FNet [39], and MGL [44], whose implementations are publicly available. In PMG, any conventional method can be incorporated as a COD model, and the performance of our method is to improve the COD model to become a more powerful one.

3.2 Pseudo-Edge Generator (PEG)

PEG is a module that outputs a pseudo-edge label E_{pseudo} from an RGB image I . To achieve this, we need to train some kind of edge detection model suitable for the camouflaged object datasets. However, most of the objects in the datasets handled by existing edge detection models are salient objects, and they cannot perform well on camouflaged objects. To deal with this problem and perform camouflaged edge detection, we follow CENet [13], which extracts the context of the input image via DAC blocks [13] and RMP blocks [13]. This is based on the hypothesis that, medical image analysis and COD are two very close tasks, in which the object in a medical image is also not salient [10]. Therefore, it is

intuitive to apply CENet to the case where the object is concealed, which fully considers semantic information of images.

The DAC block contains four cascading branches that gradually increase the number of atrous convolutions, formulated as:

$$y[i] = \sum_k x[i + rk]w[k], \quad (1)$$

where the convolution of the input feature map x and a filter w yields the output y , and the atrous rate r corresponds to the stride at which the input signal is sampled. Therefore, the DAC block can extract features from different scales. In the RMP block, after gathering context information with four different sizes of pooling kernels, features are fed into 1×1 convolution and combined with the original features. Using these blocks, the semantic information of the context is extracted and we can achieve a high-level feature map. We use binary cross-entropy (BCE) loss to train the PEG. However, according to our observation through experiment, directly using the classical BCE loss will face the problem of overfitting. To mitigate this, we introduce a new edge loss with Flooding [18] that is calculated as:

$$\mathcal{L}_{\text{edge}} = |\mathcal{L}_{\text{bce}}(E_{\text{pseudo}}, E_{\text{GT}}) - b| + b, \quad (2)$$

where b is the flooding level, which sets the target value of loss to a small constant.

3.3 Uncertainty-Aware Map Refinement Module (UAMR)

To obtain the clear boundaries, we introduce a refinement module to refine the obscure boundaries of pseudo-map labels M_{pseudo} generated from PMG together using pseudo-edge labels E_{pseudo} generated from PEG. However, these pseudo labels are predicted by the learning-based model, and thus contain uncertainty. Inspired by UCNNet [45], we propose a UAMR module that can absorb uncertainty. Similar to [45], we assume that pseudo-map labels and pseudo-edge labels have similar properties as depth labels in that they provide clues for object detection. By extending UCNNet to support pseudo-map labels and pseudo-edge labels, we construct the UAMR module that considers uncertainty. Therefore, the input to the UAMR module is an RGB image I , a pseudo-map label M_{pseudo} , and a pseudo-edge label E_{pseudo} , which are used to predict an edge-accurate camouflaged map M_{pred} . As shown in Figure 2, the UAMR module consists of PriorNet, PosteriorNet, and RefinementNet.

PriorNet takes the RGB image I , the pseudo-map label M_{pseudo} , and the pseudo-edge label E_{pseudo} as input and maps them to a low-dimensional latent variable z^{prior} . On the other hand, PosteriorNet takes all the input from PriorNet together with the ground-truth map label M_{GT} as input and maps them to a low-dimensional latent variable z^{post} . Note that PriorNet and PosteriorNet form CVAE, and each latent variable $z^{\text{prior}}, z^{\text{post}}$ is sampled from the Gaussian distribution consisting of the parameters of the output mean $\mu^{\text{prior}}, \mu^{\text{post}}$ and variance $\sigma^{\text{prior}}, \sigma^{\text{post}}$. As for the CVAE loss, let X denotes $(I, M_{\text{pseudo}}, E_{\text{pseudo}})$, let Y denotes the ground-truth map M_{GT} . The PriorNet is defined as $P_{\theta}(z^{\text{prior}} | X)$ and the PosteriorNet is defined as $Q_{\phi}(z^{\text{post}} | X, Y)$, where θ is the parameter set of PriorNet and ϕ is that of PosteriorNet. The CVAE loss is defined as:

$$\begin{aligned} \mathcal{L}_{\text{CVAE}} = & E_{z \sim Q_{\phi}(z^{\text{post}} | X, Y)} [-\log P_{\omega}(Y | X, z^{\text{post}})] \\ & + D_{\text{KL}}(Q_{\phi}(z^{\text{post}} | X, Y) \parallel P_{\theta}(z^{\text{prior}} | X)), \end{aligned} \quad (3)$$

where $P_{\omega}(Y | X, z^{\text{post}})$ is the likelihood of $P(Y)$ given latent variable z^{post} and conditioning variable X , and D_{KL} is Kullback-Leibler Divergence.

RefinementNet takes the RGB image I , the pseudo-map label M_{pseudo} , the pseudo-edge label E_{pseudo} , and each latent variable $z^{\text{prior}}, z^{\text{post}}$ as input, which is trained to estimate the camouflaged map M_{pred} , the corrected pseudo-edge label E_{ref} , and the corrected pseudo-map label M_{ref} . Therefore, using the latent variables in CVAE, we can consider the uncertainty of the pseudo-map labels and pseudo-edge labels by learning to make the reconstructed pseudo-map label M_{ref} closer to the ground-truth M_{GT} and the reconstructed pseudo-edge label E_{ref} closer to the ground-truth edge label E_{GT} . As for the loss for RefinementNet, MSE loss \mathcal{L}_{mse} , smoothness loss [12] $\mathcal{L}_{\text{smooth}}$, and structure loss [26] $\mathcal{L}_{\text{struct}}$ are used. Smoothness loss is used to enhance the structure information in the image, while structure loss is used to enforce spatial coherence of the prediction and using both the local and global features

in the optimization. Thus, the refinement loss is defined as:

$$\begin{aligned} \mathcal{L}_{\text{ref}} = & \lambda_{\text{mse}}^{\text{prior}} \mathcal{L}_{\text{mse}}(P_{\text{ref}}^{\text{prior}}, P_{\text{GT}}^{\text{prior}}) + \lambda_{\text{mse}}^{\text{post}} \mathcal{L}_{\text{mse}}(P_{\text{ref}}^{\text{post}}, P_{\text{GT}}^{\text{post}}) \\ & + \lambda_{\text{smooth}}^{\text{prior}} \mathcal{L}_{\text{smooth}}(M_{\text{pred}}^{\text{prior}}, M_{\text{GT}}) + \lambda_{\text{smooth}}^{\text{post}} \mathcal{L}_{\text{smooth}}(M_{\text{pred}}^{\text{post}}, M_{\text{GT}}) \\ & + \lambda_{\text{struct}}^{\text{prior}} \mathcal{L}_{\text{struct}}(M_{\text{pred}}^{\text{prior}}, M_{\text{GT}}) + \lambda_{\text{struct}}^{\text{post}} \mathcal{L}_{\text{struct}}(M_{\text{pred}}^{\text{post}}, M_{\text{GT}}), \end{aligned} \quad (4)$$

where P denotes (M, E) , and λ denotes the weight for each loss.

Finally, combing the above three modules together, we get the overall loss for our model:

$$\mathcal{L} = \lambda_{\text{edge}} \mathcal{L}_{\text{edge}} + \lambda_{\text{CVAE}} \mathcal{L}_{\text{CVAE}} + \lambda_{\text{ref}} \mathcal{L}_{\text{ref}}, \quad (5)$$

where λ denotes the weight for each loss. In testing, the output camouflaged map $M_{\text{pred}}^{\text{prior}}$ of RefinementNet is treated as the final output of our framework.

4 EXPERIMENTS

4.1 Experimental Settings

4.1.1 Implementation Details. We implement our model using PyTorch, and initialized the encoder of RefinementNet with ResNet-50 [15] parameters pre-trained on ImageNet and the encoder of PEG with the parameters of ResNet-34 [15]. We resize all the images to 352×352 for both training and testing. The scale of latent space is set to 3, and the maximum epoch is 100. We optimize the overall parameters using the Adam algorithm, where the initial learning rate is 5e-5 and after 80 epochs, the learning rate is reduced by 10% for each epoch. The whole training takes 8.5 hours with batch size 10 on an NVIDIA Tesla V100 GPU. Besides, our approach has a low computational cost during the inference.

4.1.2 Datasets. To train our framework, we used a standard training dataset for COD which contains 3,040 images from the COD10K dataset [9] and 1,000 images from CAMO dataset [20]. During training, we generated the ground-truth edge labels from the ground-truth map labels. To evaluate our framework, we used the CAMO dataset consisting of 250 images with camouflaged objects, the CHAMELEON dataset [34] consisting of 76 images, the COD10K dataset consisting of 2,026 images, and the NC4K dataset [27] consisting of 4,121 images.

4.1.3 Evaluation Metrics. Four quantitative evaluation metrics are widely used to evaluate the performance of CODs: Mean Absolute Error (MAE), S-measure [6], E-measure [7], and weighted F-measure [28] denoted as \mathcal{M} , S_{α} , E_{ϕ} , and F_{β}^w , respectively.

\mathcal{M} is defined as per-pixel-wise difference between the predicted map M_{pred} and the ground-truth map M_{GT} as: $\mathcal{M} = \frac{1}{H \times W} | M_{\text{pred}} - M_{\text{GT}} |$, where H and W are the height and width of M_{pred} . The MAE directly evaluates the conformity between the estimated map and the ground-truth map. S-measure S_{α} is a structure-based metric that combines region-aware structural similarity S_r and object-aware structural similarity S_o as: $S_{\alpha} = \alpha S_o + (1 - \alpha) S_r$, and the balance parameter α is set to 0.5 as default. E-measure E_{ϕ} simultaneously evaluates the local pixel-level matching information and the image-level statistics. Weighted F-measure F_{β}^w defines a weighted precision that can provide more reliable evaluation results than F-measure, which is a comprehensive measure of both precision and recall of the predicted camouflaged map.

Table 1: Quantitative results on four standard COD datasets. \uparrow indicates the higher the score the better, and vice versa.

Methods	CHAMELEON				CAMO-Test				COD10K-Test				NC4K			
	$S_\alpha \uparrow$	$E_\phi \uparrow$	$F_\beta^w \uparrow$	$M \downarrow$	$S_\alpha \uparrow$	$E_\phi \uparrow$	$F_\beta^w \uparrow$	$M \downarrow$	$S_\alpha \uparrow$	$E_\phi \uparrow$	$F_\beta^w \uparrow$	$M \downarrow$	$S_\alpha \uparrow$	$E_\phi \uparrow$	$F_\beta^w \uparrow$	$M \downarrow$
FPN [21]	0.794	0.783	0.590	0.075	0.684	0.677	0.483	0.131	0.697	0.691	0.411	0.075	-	-	-	-
MaskRCNN [14]	0.643	0.778	0.518	0.099	0.574	0.715	0.430	0.151	0.613	0.748	0.402	0.080	-	-	-	-
PSPNet [47]	0.773	0.758	0.555	0.085	0.663	0.659	0.455	0.139	0.678	0.680	0.377	0.080	-	-	-	-
UNet++ [50]	0.695	0.762	0.501	0.094	0.599	0.653	0.392	0.149	0.623	0.672	0.350	0.086	-	-	-	-
PiCANet [23]	0.769	0.749	0.536	0.085	0.609	0.584	0.356	0.156	0.649	0.643	0.322	0.090	-	-	-	-
MSRCNN [17]	0.637	0.686	0.443	0.091	0.617	0.669	0.454	0.133	0.641	0.706	0.419	0.073	-	-	-	-
PFANet [49]	0.679	0.648	0.378	0.144	0.659	0.622	0.391	0.172	0.636	0.618	0.286	0.128	-	-	-	-
CPD [41]	0.853	0.866	0.706	0.052	0.726	0.729	0.550	0.115	0.747	0.770	0.508	0.059	-	-	-	-
HTC [3]	0.517	0.489	0.204	0.129	0.476	0.442	0.174	0.172	0.548	0.520	0.221	0.088	-	-	-	-
ANet-SRM [20]	-	-	-	-	0.682	0.685	0.484	0.126	-	-	-	-	-	-	-	-
EGNet [48]	0.848	0.870	0.702	0.050	0.732	0.768	0.583	0.104	0.737	0.779	0.509	0.056	-	-	-	-
MirrorNet [43]	-	-	-	-	0.741	0.804	0.652	0.100	-	-	-	-	-	-	-	-
TIGNet [51]	0.874	0.916	0.783	0.038	0.781	0.847	0.678	0.087	0.793	0.848	0.635	0.043	-	-	-	-
PFNet [29]	0.882	-	0.810	0.033	0.782	-	0.695	0.085	0.800	-	0.660	0.040	-	-	-	-
LSR [27]	0.893	0.938	-	0.033	0.793	0.826	-	0.085	0.793	0.868	-	0.041	0.839	0.883	-	0.053
SINet [9]	0.872	0.936	0.806	0.034	0.745	0.804	0.644	0.092	0.776	0.864	0.631	0.043	0.808	0.871	0.723	0.058
UR-SINet (Ours)	0.876	0.942	0.824	0.031	0.741	0.804	0.649	0.091	0.775	0.869	0.643	0.041	0.806	0.873	0.731	0.057
PraNet [10]	0.860	0.907	0.763	0.044	0.769	0.824	0.663	0.094	0.789	0.861	0.629	0.045	0.822	0.876	0.724	0.059
UR-PraNet (Ours)	0.884	0.936	0.835	0.032	0.762	0.831	0.679	0.089	0.790	0.877	0.661	0.039	0.820	0.885	0.747	0.054
C ² FNet [39]	0.888	0.935	0.828	0.032	0.796	0.854	0.719	0.080	0.813	0.890	0.686	0.036	0.839	0.897	0.766	0.049
UR-C ² FNet (Ours)	0.889	0.940	0.844	0.029	0.791	0.856	0.725	0.079	0.811	0.897	0.700	0.034	0.836	0.900	0.775	0.047
MGL [44]	0.892	0.913	0.802	0.032	0.772	0.807	0.664	0.089	0.811	0.844	0.654	0.037	0.829	0.863	0.730	0.055
UR-MGL (Ours)	0.891	0.942	0.844	0.026	0.763	0.824	0.682	0.086	0.803	0.879	0.685	0.034	0.821	0.882	0.752	0.051
SINet-v2 [8]	0.888	0.942	0.816	0.030	0.820	0.882	0.743	0.070	0.815	0.887	0.680	0.037	0.847	0.903	0.770	0.048
UR-SINet-v2 (Ours)	0.901	0.960	0.862	0.023	0.814	0.891	0.758	0.067	0.816	0.903	0.708	0.033	0.844	0.910	0.787	0.045

Table 2: Ablation experiments of the proposed model.

Methods	CHAMELEON				CAMO-Test				COD10K-Test				NC4K			
	$S_\alpha \uparrow$	$E_\phi \uparrow$	$F_\beta^w \uparrow$	$M \downarrow$	$S_\alpha \uparrow$	$E_\phi \uparrow$	$F_\beta^w \uparrow$	$M \downarrow$	$S_\alpha \uparrow$	$E_\phi \uparrow$	$F_\beta^w \uparrow$	$M \downarrow$	$S_\alpha \uparrow$	$E_\phi \uparrow$	$F_\beta^w \uparrow$	$M \downarrow$
SINet-v2 [8]	0.888	0.942	0.816	0.030	0.820	0.882	0.743	0.070	0.815	0.887	0.680	0.037	0.847	0.903	0.770	0.048
UR-SINet-v2 w/o PEG	0.898	0.957	0.857	0.024	0.813	0.890	0.756	0.068	0.814	0.902	0.704	0.034	0.842	0.909	0.784	0.046
UR-SINet-v2 w/o PMG	0.873	0.919	0.814	0.038	0.705	0.737	0.571	0.105	0.742	0.805	0.573	0.047	0.786	0.841	0.687	0.063
UR-SINet-v2 (Ours)	0.901	0.960	0.862	0.023	0.814	0.891	0.758	0.067	0.816	0.903	0.708	0.033	0.844	0.910	0.787	0.045

4.2 Comparison with State-of-the-arts

We compare our method against 20 state-of-the-art baselines: object detection method FPN [21]; semantic segmentation method PSPNet [47]; instance segmentation methods MaskRCNN [14], HTC [3], and MSRCNN [17]; medical image segmentation methods UNet++ [50] and PraNet [10]; salient object detection methods PiCANet [23], CPD [41], PFANet [49], EGNet [48]; and COD methods ANet-SRM [20], SINet [9], MirrorNet [43], C²FNet [39], TIGNet [51], PFNet [29], MGL [44], LSR [27], SINet-v2 [8]. For a fair comparison, the results of the non-COD methods are taken from [8], and the results of the COD methods are taken from the respective papers, some of which are obtained by output camouflaged maps provided on public websites or running models retrained with open source code.

4.3 Quantitative Evaluation

Table 1 shows the metric scores of the proposed method and 20 state-of-the-art baselines on the four benchmark datasets. We can see that our method of "UR-SINet-v2 (Ours)" outperforms almost all

the other methods on four standard metrics: S-measure, E-measure, weighted F-measure, and MAE, which achieves average improvements of 0.13%, 3.5%, 1.4%, and 11.2%, respectively, when compared to the SINet-v2. Moreover, although the performance of the S-measure is slightly lower, the overall scores of the other metrics are significantly improved compared to the original COD methods without our framework, due to considering the uncertainty of pseudo-edge labels and pseudo-map labels. The reason why the score of S-measure is slightly low is that the output camouflaged maps of our method have clear boundaries, and the penalty for failing to predict the true camouflaged maps is much larger for S-measure, which measures structural similarity, than for the case where the boundaries are ambiguous.

4.4 Visualization

Figure 3 shows the visual examples that are generated by our method and compared methods. We can see that the camouflaged map is refined by appropriately combining the information of the pseudo-map label and the pseudo-edge label. In particular, details

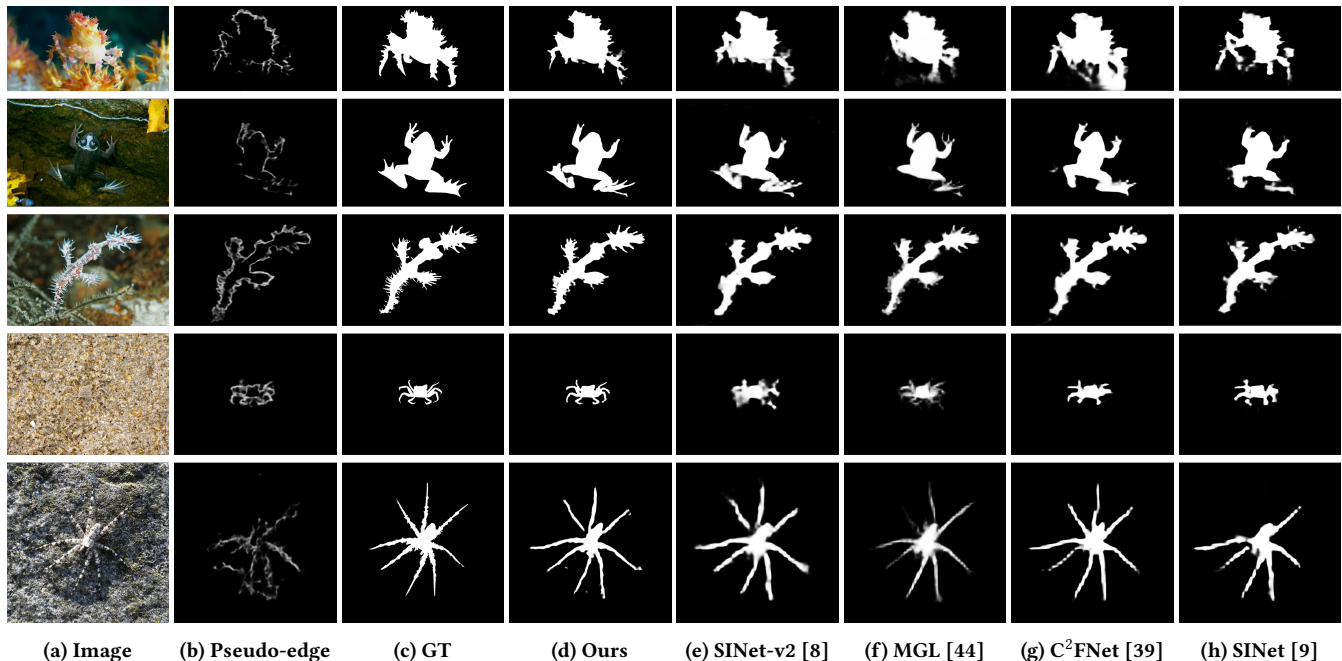


Figure 3: Visual comparison of the proposed model with state-of-the-art methods. "UR-SINet-v2" model is adopted as our model (d), and (e) is also used as a pseudo-map label for training our model. Our model outputs camouflaged maps with accurate boundaries based on the uncertain pseudo-map labels and pseudo-edge labels.

such as tactile sensation and limbs of camouflaged objects, which tend to be difficult to detect by conventional methods, can be estimated accurately by the proposed method.

4.5 Ablation Study

4.5.1 Effectiveness of Pseudo-Edge Labels. In the baseline setting, we generate pseudo-edge labels from PEG and pseudo-map labels from PMG, then input both pseudo-edge and pseudo-map labels into the UAMR module and obtain the output camouflaged maps. Table 2 shows the result of not inputting the pseudo-edge labels into the UAMR module, and the performance gets slightly lower. In our framework, the edge information helps to correct the edges of the camouflaged maps and make the details of the edges better. However, the metric scores focus on analyzing the scores of the overall effects. So, the visualization is better but the increase in scores is not obvious.

4.5.2 Effectiveness of Pseudo-Map Labels. In contrast, table 2 also shows the result of not inputting the pseudo-map labels into the UAMR module, and the performance is considerably lower. This is because pseudo-edge labels alone may not capture all the edges of camouflaged objects, and they contain a relatively large amount of uncertainty.

5 CONCLUSIONS

In this study, we dealt with camouflaged object detection, which is a challenging task to detect objects hidden in the environment. Previous COD models, that directly segment objects, often result in blurred and ambiguous boundaries of the output camouflaged

map, while models that consider edge information have slightly lower performance. To handle these problems, we aim to combine the best of both methods and propose to refine the pseudo-map labels generated from conventional COD methods by referring to the pseudo-edge labels generated from a camouflaged edge detection module. To solve the problem that pseudo-map labels and pseudo-edge labels are noisy and contain uncertainty, we proposed an uncertainty-aware map refinement module that outputs edge-accurate camouflaged maps. We conducted a quantitative evaluation on the standard four COD datasets and found that the proposed method outperformed the state-of-the-art methods in almost all of the four evaluation metrics.

REFERENCES

- [1] Gedas Bertasius, Jianbo Shi, and Lorenzo Torresani. 2015. Deepedge: A multi-scale bifurcated deep network for top-down contour detection. In *CVPR*. 4380–4389.
- [2] John Canny. 1986. A computational approach to edge detection. *TPAMI* 6 (1986), 679–698.
- [3] Kai Chen, Jiangmiao Pang, Jiaqi Wang, Yu Xiong, Xiaoxiao Li, Shuyang Sun, Wansen Feng, Ziwei Liu, Jianping Shi, Wanli Ouyang, et al. 2019. Hybrid task cascade for instance segmentation. In *CVPR*. 4974–4983.
- [4] Innes C Cuthill, Martin Stevens, Jenna Sheppard, Tracey Maddocks, C Alejandro Párraga, and Tom S Troscianko. 2005. Disruptive coloration and background pattern matching. *Nature* 434, 7029 (2005), 72–74.
- [5] John Egan, Rebecca J Sharman, Kenneth C Scott-Brown, and Paul George Lovell. 2016. Edge enhancement improves disruptive camouflage by emphasising false edges and creating pictorial relief. *Scientific reports* 6, 1 (2016), 1–9.
- [6] Deng-Ping Fan, Ming-Ming Cheng, Yun Liu, Tao Li, and Ali Borji. 2017. Structure-measure: A new way to evaluate foreground maps. In *ICCV*. 4548–4557.
- [7] Deng-Ping Fan, Cheng Gong, Yang Cao, Bo Ren, Ming-Ming Cheng, and Ali Borji. 2018. Enhanced-alignment measure for binary foreground map evaluation. In *IJCAI*. 698–704.
- [8] Deng-Ping Fan, Ge-Peng Ji, Ming-Ming Cheng, and Ling Shao. 2021. Concealed Object Detection. *IEEE TPAMI* (2021).

- [9] Deng-Ping Fan, Ge-Peng Ji, Guolei Sun, Ming-Ming Cheng, Jianbing Shen, and Ling Shao. 2020. Camouflaged object detection. In *CVPR*. 2777–2787.
- [10] Deng-Ping Fan, Ge-Peng Ji, Tao Zhou, Geng Chen, Huazhu Fu, Jianbing Shen, and Ling Shao. 2020. Pranet: Parallel reverse attention network for polyp segmentation. In *MICCAI*. 263–273.
- [11] Jaime Gallego and Pascal Bertolino. 2014. Foreground object segmentation for moving camera sequences based on foreground-background probabilistic models and prior probability maps. In *ICIP*. 3312–3316.
- [12] Clément Godard, Oisín Mac Aodha, and Gabriel J Brostow. 2017. Unsupervised monocular depth estimation with left-right consistency. In *CVPR*. 270–279.
- [13] Zaiwang Gu, Jun Cheng, Huazhu Fu, Kang Zhou, Huaying Hao, Yitian Zhao, Tianyang Zhang, Shenghua Gao, and Jiang Liu. 2019. Ce-net: Context encoder network for 2d medical image segmentation. *TMI* (2019).
- [14] Kaiming He, Georgia Gkioxari, Piotr Dollar, and Ross Girshick. 2017. Mask R-CNN. In *ICCV*.
- [15] Kaiming He, Xiangyu Zhang, Shaoqing Ren, and Jian Sun. 2016. Deep residual learning for image recognition. In *CVPR*. 770–778.
- [16] Jianqin Yin Yanbin Han Wendi Hou and Jinping Li. 2011. Detection of the mobile object with camouflage color under dynamic background based on optical flow. *Procedia Engineering* 15 (2011), 2201–2205.
- [17] Zhaojin Huang, Lichao Huang, Yongchao Gong, Chang Huang, and Xinggong Wang. 2019. Mask scoring r-cnn. In *CVPR*. 6409–6418.
- [18] Takashi Ishida, Ikko Yamane, Tomoya Sakai, Gang Niu, and Masashi Sugiyama. 2020. Do We Need Zero Training Loss After Achieving Zero Training Error? *ICML* (2020).
- [19] Ch Kavitha, B Prabhakara Rao, and A Govardhan. 2011. An efficient content based image retrieval using color and texture of image sub-blocks. *IJEST* 3, 2 (2011), 1060–1068.
- [20] Trung-Nghia Le, Tam V Nguyen, Zhongliang Nie, Minh-Triet Tran, and Akihiro Sugimoto. 2019. Anabranch network for camouflaged object segmentation. *CVIU* 184 (2019), 45–56.
- [21] Tsung-Yi Lin, Piotr Dollár, Ross Girshick, Kaiming He, Bharath Hariharan, and Serge Belongie. 2017. Feature pyramid networks for object detection. In *CVPR*. 2117–2125.
- [22] Li Liu, Wanli Ouyang, Xiaogang Wang, Paul Fieguth, Jie Chen, Xinwang Liu, and Matti Pietikäinen. 2020. Deep learning for generic object detection: A survey. *IJCV* 128, 2 (2020), 261–318.
- [23] Nian Liu, Junwei Han, and Ming-Hsuan Yang. 2018. Picanet: Learning pixel-wise contextual attention for saliency detection. In *CVPR*. 3089–3098.
- [24] Yun Liu, Ming-Ming Cheng, Xiaowei Hu, Kai Wang, and Xiang Bai. 2017. Richer convolutional features for edge detection. In *CVPR*. 3000–3009.
- [25] Zhou Liu, Kaiqi Huang, and Tieniu Tan. 2012. Foreground object detection using top-down information based on EM framework. *TIP* 21, 9 (2012), 4204–4217.
- [26] Zhiming Luo, Akshaya Mishra, Andrew Achkar, Justin Eichel, Shaozi Li, and Pierre-Marc Jodoin. 2017. Non-local deep features for salient object detection. In *CVPR*. 6609–6617.
- [27] Yunqiu Lyu, Jing Zhang, Yuchao Dai, Aixuan Li, Bowen Liu, Nick Barnes, and Deng-Ping Fan. 2021. Simultaneously Localize, Segment and Rank the Camouflaged Objects. In *CVPR*.
- [28] Ran Margolin, Lihl Zelnik-Manor, and Ayellet Tal. 2014. How to evaluate foreground maps?. In *CVPR*. 248–255.
- [29] Haiyang Mei, Ge-Peng Ji, Ziqi Wei, Xin Yang, Xiaopeng Wei, and Deng-Ping Fan. 2021. Camouflaged object segmentation with distraction mining. In *CVPR*. 8772–8781.
- [30] D Osorio and MV Srinivasan. 1991. Camouflage by edge enhancement in animal coloration patterns and its implications for visual mechanisms. *Proceedings of the Royal Society of London. Series B: Biological Sciences* 244, 1310 (1991), 81–85.
- [31] Yuxin Pan, Yiwang Chen, Qiang Fu, Ping Zhang, and Xin Xu. 2011. Study on the camouflaged target detection method based on 3D convexity. *Modern Applied Science* 5, 4 (2011), 152.
- [32] P Sengottuvelan, Amitabh Wahi, and A Shanmugam. 2008. Performance of decamouflaging through exploratory image analysis. In *ICETET*. 6–10.
- [33] P Siricharoen, S Aramvith, TH Chalidabhongse, and S Siddhichai. 2010. Robust outdoor human segmentation based on color-based statistical approach and edge combination. In *ICGCS*. 463–468.
- [34] P Skurowski, H Abdulameer, J Błaszczyk, T Depta, A Kornacki, and P Koziel. 2018. Animal camouflage analysis: Chameleon database. *Unpublished Manuscript* (2018).
- [35] Kihyuk Sohn, Honglak Lee, and Xinchen Yan. 2015. Learning structured output representation using deep conditional generative models. *NeurIPS* 28 (2015), 3483–3491.
- [36] Liming Song and Weidong Geng. 2010. A new camouflage texture evaluation method based on WSSIM and nature image features. In *ICMT*. 1–4.
- [37] Xavier Soria, Edgar Riba, and Angel Sappa. 2020. Dense Extreme Inception Network: Towards a Robust CNN Model for Edge Detection. In *WACV*.
- [38] Martin Stevens and Sami Merilaita. 2009. Animal camouflage: current issues and new perspectives. *Philosophical Transactions of the Royal Society B: Biological Sciences* 364, 1516 (2009), 423–427.
- [39] Yujia Sun, Geng Chen, Tao Zhou, Yi Zhang, and Nian Liu. 2021. Context-aware Cross-level Fusion Network for Camouflaged Object Detection. *arXiv* (2021).
- [40] Wenguan Wang, Shuyang Zhao, Jianbing Shen, Steven CH Hoi, and Ali Borji. 2019. Salient object detection with pyramid attention and salient edges. In *CVPR*. 1448–1457.
- [41] Zhe Wu, Li Su, and Qingming Huang. 2019. Cascaded partial decoder for fast and accurate salient object detection. In *CVPR*. 3907–3916.
- [42] Saining Xie and Zhuowen Tu. 2015. Holistically-nested edge detection. In *ICCV*. 1395–1403.
- [43] Jinnan Yan, Trung-Nghia Le, Khanh-Duy Nguyen, Minh-Triet Tran, Thanh-Toan Do, and Tam V Nguyen. 2020. MirrorNet: Bio-Inspired Adversarial Attack for Camouflaged Object Segmentation. *arXiv* (2020).
- [44] Qiang Zhai, Xin Li, Fan Yang, Chenglizhao Chen, Hong Cheng, and Deng-Ping Fan. 2021. Mutual Graph Learning for Camouflaged Object Detection. In *CVPR*.
- [45] Jing Zhang, Deng-Ping Fan, Yuchao Dai, Saeed Anwar, Fatemeh Sadat Saleh, Tong Zhang, and Nick Barnes. 2020. UC-Net: Uncertainty inspired RGB-D saliency detection via conditional variational autoencoders. In *CVPR*. 8582–8591.
- [46] Jing Zhang, Yunqiu Lv, Mochu Xiang, Aixuan Li, Yuchao Dai, and Yiran Zhong. 2021. Depth Confidence-aware Camouflaged Object Detection. *arXiv* (2021).
- [47] Hengshuang Zhao, Jianping Shi, Xiaojuan Qi, Xiaogang Wang, and Jiaya Jia. 2017. Pyramid scene parsing network. In *CVPR*. 2881–2890.
- [48] Jia-Xing Zhao, Jiang-Jiang Liu, Deng-Ping Fan, Yang Cao, Jufeng Yang, and Ming-Ming Cheng. 2019. EGNNet: Edge guidance network for salient object detection. In *ICCV*. 8779–8788.
- [49] Ting Zhao and Xiangqian Wu. 2019. Pyramid feature attention network for saliency detection. In *CVPR*. 3085–3094.
- [50] Zongwei Zhou, Md Mahfuzur Rahman Siddiquee, Nima Tajbakhsh, and Jianming Liang. 2018. Unet++: A nested u-net architecture for medical image segmentation. In *DLMIA*. 3–11.
- [51] Jinchao Zhu, Xiaoyu Zhang, Shuo Zhang, and Junnan Liu. 2021. Inferring Camouflaged Objects by Texture-Aware Interactive Guidance Network. In *AAAI*, Vol. 35. 3599–3607.